**Life Estimation of High Level Waste Tank Steel for F-Tank Farm Closure Performance Assessment - 9310**

K.H. Subramanian
Washington Savannah River Company
URS-Washington Division
Bldg 766-H, Aiken SC 29808

B.J. Wiersma, S.P. Harris
Savannah River National Laboratory
Bldg 773-A, Aiken SC 29808

**ABSTRACT**

High level radioactive waste (HLW) is stored in underground carbon steel storage tanks at the Savannah River Site. The underground tanks will be closed by removing the bulk of the waste, chemical cleaning, heel removal, stabilizing remaining residuals with tailored grout formulations, and severing/sealing external penetrations. The life of the carbon steel materials of construction in support of the performance assessment has been completed. The estimation considered general and localized corrosion mechanisms of the tank steel exposed to grouted conditions. A stochastic approach was followed to estimate the distributions of failures based upon mechanisms of corrosion accounting for variances in each of the independent variables. The methodology and results used for one-type of tank is presented.

**INTRODUCTION**

High level radioactive waste (HLW) is stored in underground storage tanks at the Savannah River Site. Closure of these tanks consists of removing the bulk of the waste, chemical cleaning, heel removal, and filling the tank with tailored grout formulations and severing/sealing external penetrations. A performance assessment is being developed in support of closure and requires an accurate assessment of the corrosion of the materials of construction. Initially, the carbon steel construction materials of the high level waste tanks will provide a barrier to the leaching of radionuclides into the soil. However, the carbon steel liners will degrade over time, most likely due to corrosion, and no longer provide a barrier. The corrosion assessment of the high level waste tank primary and secondary tanks will provide the necessary inputs for the radionuclide transport modeling. The corrosion assessment began with the expected initial condition of each of the tanks at closure, and considered general and pitting corrosion once grouted.

The tanks are a steel-lined pre-stressed concrete tank in the form of a vertical cylinder with a domed roof (Fig. 1). Each tank is 85 feet in diameter, 34 feet high and has a capacity of 1,300,000 gallons. The walls and bottom of the liner are constructed of low carbon steel plate, 0.375-in. thick. The lower knuckle joining the wall and bottom is made of 0.4375-in. thick low carbon steel.
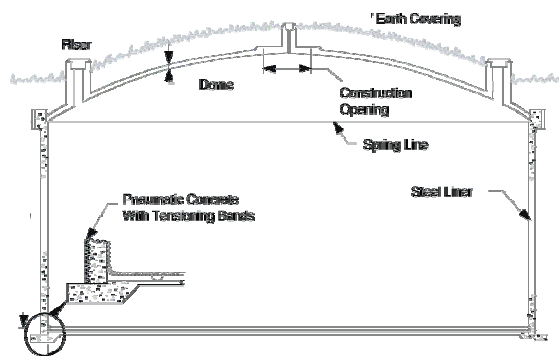
**Fig. 1: High Level Radioactive Waste Tank.**

The steel liners were constructed of ASTM A285 steel, the nominal composition of which is shown in Table 1.

**Table 1: ASTM Requirements for Chemical Composition for A285-50T, Grade B Firebox Quality[1]**

| | Composition, wt. % | | | |
|---|---|---|---|---|
| For plates ≤ 0.75" thickness | $C_{max}$ | $Mn_{max}$ | $P_{max}$ | $S_{max}$ |
| | 0.2* | 0.8 | 0.035 | 0.04 |

*C = 0.22 wt.% for plate of 0.75"< thickness ≤ 2"

## LIFE ESTIMATION METHODOLOGY

The life of the tank steels and performance as a barrier to radionuclide escape is dependent upon the active corrosion mechanisms on the steel under closure conditions. Corrosion was calculated based upon specific exposures of the tank steel in the closure condition. A stochastic approach to the life estimation of the tanks was developed to provide a tool to confidently prove that regulatory compliance is being met. The stochastic methods are proposed to account for potential uncertainty in the time-frames proposed for regulatory compliance. The Monte Carlo approach was determined to be the most appropriate for time-to-failure estimation of the tank liner due to its ability to inherently represent the uncertainties in the deterministic approach and also allow for a large number of simulations. In addition, the Monte-Carlo approach exploits the in-depth knowledge of SRS subsurface environments and HLW tanks as input distributions for the simulations.

### Corrosion Mechanisms in Concrete/Grout

Corrosion of steel exposed to concrete/grout occurs by a complex mechanism through metal dissolution at the concrete/metal interface. This interfacial chemistry is controlled by the initial construction characteristics and the grout formulations. In general, high quality concrete prevents corrosion of the steel by: (1) forming a passive oxide on the steel surface, (2) maintaining a high pH environment, and (3) providing a matrix resistant to diffusion of aggressive species. The passivity of the steel at the interface can be controlled by the dynamic characteristics of the "pore water" (interstitial solution) within the concrete.[2] The passivity is maintained at the high pH environments in the region of water stability. However, as pore water characteristics change with the introduction of chlorides or carbon dioxide, the passive film on the steel may break down. The two major causes of corrosion of steel exposed to concrete are carbonation and chloride induced breakdown of the passive film. The passivity of the steel is lost

when the pH is lowered below 9 (by carbonation) or a critical chloride concentration is reached at the concrete metal interface.[3]

The initial concrete material quality is potentially the most significant factor in the prevention of corrosion of the steel in contact with as-constructed vault. The tanks have a concrete vault that was formed by the "shotcrete" technique [4] The cement density, water-to-cement (WCR) ratio, and content are key parameters for cement content and type. The cement density of the mixture has been calculated to be 590 lbs/yd$^3$, consistently above the minimum 490 lbs/yd$^3$.[5] The water to cement ratio was calculated to be 0.6, which is relatively high. However, water proofing membranes were used in the HLW tanks to prevent chloride intrusion from external sources. The concrete may have been constructed with either Portland cement, 75% Portland cement with 25% slag cement, or 85% Portland cement and 15% fly ash. The use of blended cements may affect the corrosion rate due to reduced alkalinity. However, these cements also decrease the permeability to anions that potentially cause pitting in the steel, i.e. chloride by reducing the water to cement ratio.[6]

It is assumed in this case that a passive layer forms on the steel surface spontaneously when in contact with the alkaline cement. This corrosion rate in this inactive state is estimated to be 0.04 mils/year (1µm/year). [7] This corrosion rate corresponds to a passive current density ($I_{corr}$) of 0.09 µA/cm$^2$, which is just below the typical threshold used for the passive state, i.e. $I_{corr} < 0.1$ µA/cm$^2$.[8] The technical basis for the corrosion rate distribution is discussed later.

## TECHNICAL APPROACH

Life of the tank liners was assumed to be a function of the time to corrosion initiation plus the time for corrosion to propagate through the liner. The corrosion proceeds under grouted conditions, until chloride can induce depassivation of the surface, or carbonation can reduce the pH of the surrounding concrete thereby negating the high pH "protection" of the steel liner.

The failure time of the liner is defined to be:

$$t_{failure} = t_{initiation} + \frac{Thickness(mils)}{CorrosionRate(mils/year)}$$

where: 
| | | |
|---|---|---|
| $t_{failure}$ | = | time to complete consumption of tank wall by general corrosion |
| $t_{initiation}$ | = | time to chloride induced depassivation or carbonation front |
| Thickness | = | initial thickness of liner (mils) |
| Corrosion rate: | = | Dependent upon condition, i.e. chloride or carbonation |

The time to failure of the liner by general corrosion can be due to (1) general corrosion in grouted conditions, (2) chloride induced depassivation, followed by general corrosion, (3) carbonation induced loss of protective capacity of the concrete, or (4) a combination. The corrosion rate once chloride induced depassivation occurs is calculated based upon the oxygen diffusion through the concrete. The corrosion rate once the carbonation front reaches the liner is assumed to be 10 mils/year. Thus the system was modeled as a competition between the initiation time to chloride induced depassivation and the initiation time to carbonation induced greater corrosion rates. The system also addressed the issue of the carbonation front reaching the tank liner prior to complete failure by chloride induced corrosion.

### Chloride Induced Corrosion

Chloride induced corrosion is due to the breakdown of the passive film, thereby indicating that chloride diffusion is the rate controlling step for corrosion initiation. Once initiation has occurred, the oxygen

diffusion to the steel surface will control the corrosion propagation. As such, the chloride induced corrosion of the tank steel will be determined by first calculating the time to initiation, then calculating the corrosion rate. The chloride induced initiation of corrosion of steel structures encased in concrete was modeled using an empirical approach [9]:

$$t_{initiation} = \frac{129 \cdot t_c^{1.22}}{WCR \cdot [Cl^-]^{0.42}}$$

where:   $t_{initiation}$   =   time required for initiation (years)
            $t_c$   =   thickness of the concrete cover (in.)
            WCR   =   water-to-cement ratio
            [Cl⁻]   =   chloride concentration in the groundwater (ppm)

The corrosion rate of propagation can be calculated by relating oxygen diffusion through the concrete to the corrosion reaction. The oxygen diffusion through the concrete is represented by:

$$N_{O_2} = D_i \frac{C_{gw}}{\Delta X}$$

where:   $N_{O2}$   =   flux of oxygen through concrete (mol/s/cm$^2$)
            $D_i$   =   oxygen diffusion coefficient in concrete (cm$^2$/sec)
            $C_{gw}$   =   concentration of oxygen in groundwater (mol/cm$^3$)
            $\Delta X$   =   Depth of concrete (cm)

The corrosion rate can then be calculated by:

$$R_{corrosion} = \frac{4}{3} N_{O_2} \frac{M_{Fe}}{\rho_{Fe}}$$

where:   $M_{Fe}$   =   molecular weight of iron (56 g/mol)
            $\rho_{Fe}$   =   density of iron (7.86 g/cm$^3$)

The WCR was determined to be of uniform distribution with a range of a minimum of 0.55 and a maximum of 0.65.

The chloride data available from the SRS groundwater was used to develop a distribution.[10] The distribution of the chloride data is shown in Fig. 2. The lognormal distribution was found to be the best fit to the data and was used for the simulations.

| Quantiles of [Cl⁻] (ppm) | | |
|---|---|---|
| 100.0% | maximum | 31.407 |
| 99.5% | | 10.346 |
| 97.5% | | 8.874 |
| 90.0% | | 7.849 |
| 75.0% | quartile | 7.270 |
| 50.0% | median | 6.867 |
| 25.0% | quartile | 6.620 |
| 10.0% | | 6.480 |
| 2.5% | | 6.383 |
| 0.5% | | 6.327 |
| 0.0% | minimum | 6.249 |

| Mean | 7.06 |
|---|---|
| Std Dev | 0.69 |
| Std Err Mean | 0.00069 |
| upper 95% Mean | 7.06 |
| lower 95% Mean | 7.06 |
| N | 1000000 |
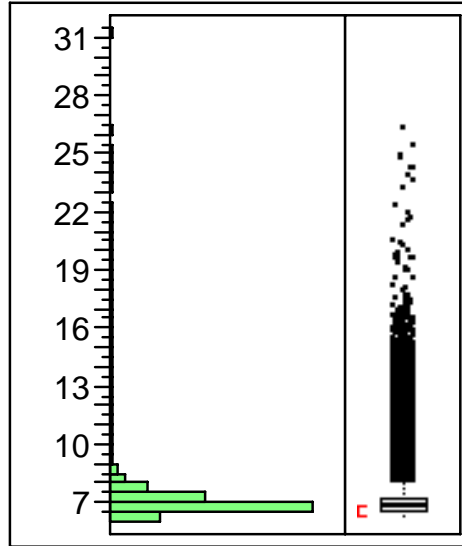


Fig. 2: Chloride Distribution per SRS Groundwater

**Corrosion by Carbonation**

Carbonation is the process through which pore water pH reduces dramatically due to the conversion of the calcium hydroxide to calcium carbonate through reaction with carbon dioxide. The active corrosion of the steel exposed to the low pH solution at the carbonation front will then proceed due to the formation of non-protective oxides.

The carbonation of concrete is a complex function of the permeability of the concrete, relative humidity, and the carbon dioxide availability. A rigorous mechanistic model for the carbonation of concrete considering mass transport, chemical reaction, and reaction kinetics has been developed.[11] The model can be simplified to the following approximation for estimation of carbonation of the tank concrete vault under the listed appropriate assumptions:[12]

$$X = \left( 2D_i \frac{C_{gw}}{C_g} \right)^{\frac{1}{2}}$$

where:

| | | | |
|---|---|---|---|
| | X | = | carbonation depth (cm) |
| | $D_i$ | = | intrinsic diffusion coefficient of $CO_2$ in concrete ($cm^2$/s) |
| | $C_{gw}$ | = | total inorganic carbon in ground water or soil moisture (mole/$cm^3$) |
| | $C_g$ | = | $Ca(OH)_2$ bulk concentration in concrete solid (mole/$cm^3$) |
| | t | = | time (s) |

This approach is appropriate for this case since subsurface concrete vaults are typically water saturated, and thus the $CO_2$ transport is in the aqueous phase. The total inorganic carbon in the groundwater was modeled based upon the data from SRS groundwater measurements, as shown in Fig. 3.[10]

| Quantiles of $[HCO_3^-]$ (mol/cm$^3$) | | |
|---|---|---:|
| 100.0% | maximum | 6.3339e-6 |
| 99.5% | | 2.3192e-6 |
| 97.5% | | 1.6157e-6 |
| 90.0% | | 1.0086e-6 |
| 75.0% | quartile | 6.06e-7 |
| 50.0% | median | 3.0338e-7 |
| 25.0% | quartile | 1.2595e-7 |
| 10.0% | | 4.5867e-8 |
| 2.5% | | 1.1e-8 |
| 0.5% | | 2.1982e-9 |
| 0.0% | minimum | 6.169e-13 |

| | |
|---|---:|
| Mean | 4.3755e-7 |
| Std Dev | 4.3775e-7 |
| Std Err Mean | 4.377e-10 |
| upper 95% Mean | 4.3841e-7 |
| lower 95% Mean | 4.367e-7 |
| N | 1000000 |
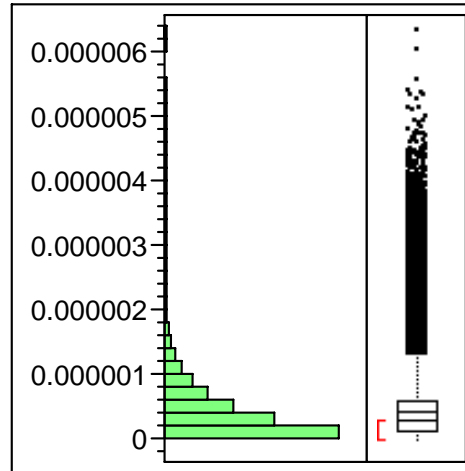
**Fig. 3: Inorganic Carbon Distribution in SRS Groundwater**

The effect of the carbonation front is essentially the reduction of the pH into a regime where the steel is susceptible to corrosion. The corrosion rate of steel exposed to aerated solutions between pH 4 and 10 is relatively independent of the pH of the environment, as shown in Fig. 4. In this pH range, the corrosion rate is governed largely by the rate at which oxygen reacts with absorbed atomic hydrogen, thereby depolarizing the surface and allowing the reduction reaction to continue. The corrosion rate within this pH range can be estimated at 10 mils/year.
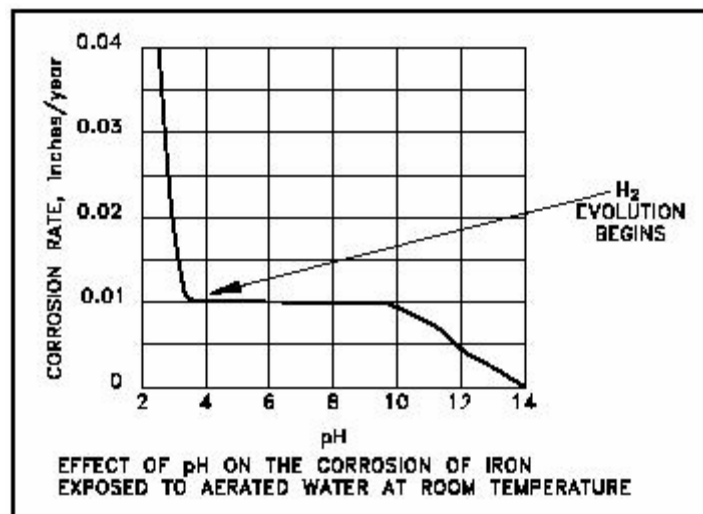
**Fig. 4: Effect of pH on the Corrosion of Iron Exposed to Aerated Water at Room Temperature [13]**

The corrosion initiation time is a function of the diffusivity of ions through the minimum dimension of the concrete vault. The thickness of the concrete was modeled using a uniform distribution for each of the tanks. The concrete cover was modeled as a uniform distribution with a 0.25-in. variation from

nominal per construction specifications.[14]  The thickness of the liner was modeled using a uniform distribution with a 0.10-in variation per construction specifications.  Steel thickness measurements made using ultrasonic techniques indicate no detectable general thinning of the waste tanks.[15]

**Distribution of Carbon Dioxide/Oxygen Diffusion Coefficients**

The distribution for the diffusion rates accounts for various scenarios that are envisioned through the concrete structure.  It is assumed that the concrete structure has some distribution of solid and pore space, which may include cracks or construction joints.  The diffusion rate is primarily assumed to be in the aqueous phase or the saturated phase of the concrete, and therefore the majority of the diffusion rate distribution falls in this region.  In addition, there is a small probability that the pore spaces may be serially connected thereby leading to a preferential pathway allowing for complete vapor space diffusion mechanisms.   The accurate determination of diffusion coefficients for mass transport through these mediums is a complex proposition and has multiple variables affecting the output.  It is typically accepted that cracking can control the mass transport through concrete structures, however, in this case, the simple thickness of the concrete structure as well as inspection knowledge of the tanks has revealed minor, if any, cracking of the concrete vault.[16]  Based upon these considerations, the distribution represented by the logarithm of the diffusion coefficient as shown in Figure 1.

| Quantiles of Diffusion Coefficients | | |
|---|---|---|
| 100.0% | maximum | -1.00 |
| 99.5% |  | -1.12 |
| 97.5% |  | -1.55 |
| 90.0% |  | -2.67 |
| 75.0% | quartile | -4.09 |
| 50.0% | median | -5.83 |
| 25.0% | quartile | -7.51 |
| 10.0% |  | -8.78 |
| 2.5% |  | -9.63 |
| 0.5% |  | -9.92 |
| 0.0% | minimum | -10.00 |

| | |
|---|---|
| Mean | -5.771115 |
| Std Dev | 2.2218854 |
| Std Err Mean | 0.0020009 |
| upper 95% Mean | -5.767193 |
| lower 95% Mean | -5.775037 |
| N | 1233023 |
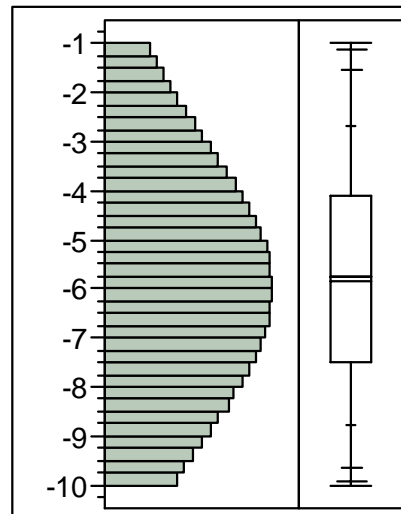


**Figure 1: Distribution of the Logarithm of Diffusion Coefficients**

The distribution is assumed to account for the various modes of diffusion possible, such as through a variety of pores, solids, and aqueous phase transport.  The broad majority of the diffusion coefficients fall within $1x10^{-9}$ cm$^2$/sec and $1x10^{-2}$ cm$^2$/sec, which is expected to encompass the majority of the regions of interest.  However the diffusion coefficients outside that regime are given lower probabilities with the higher diffusion coefficients accounting for preferential pathways and the lower coefficients accounting for diffusion through solid materials.

**CASES OF POTENTIAL CORROSION**

Three specific cases were modeled per the Monte Carlo simulation.  Carbonation induced corrosion was considered the most aggressive mechanism due to the high corrosion rate assumed, i.e. 10 mils/yr.

**Case 1: IF $t_{initiation}$ [Cl-] ≥ $t_{initiation}$ [Carbonation]**

If the time to initiation of chloride induced corrosion is greater than or equal to the time to initiation of carbonation, then carbonation was considered the controlling corrosion mechanism. Thus the time to failure was modeled as:

$$t_{failure} = t_{initiation[carbonation]} + \frac{Thickness(mils)}{CorrosionRate(mils/year)}$$

where: $T_0$          =      Initial Thickness (mils)
         Thickness      =      $T_0 - 0.04*t_{init[carbonation]}$ [mils]
         Corrosion Rate ($R_{carbonation}$)      =      10 mils/year

This then yields:

$$t_{failure} = t_{initiation[carbonation]} + \frac{T_o - \left(0.04(\frac{mils}{yr}) \cdot t_{initiation[carbonation]}\right)}{10(\frac{mils}{yr})}$$

The steel corrodes at the 0.04 mils/yr rate until the initiation of corrosion due to carbonation, followed by the increase in the corrosion rate to 10 mils/year.

**Case 2: IF $t_{initiation}$ [Cl-] < $t_{initiation}$ [Carbonation]**

If the initiation time to carbonation induced corrosion is greater than the initiation time to chloride induced corrosion, then the corrosion rate due to oxygen diffusion after chloride induced depassivation is calculated to determine the failure time. This was modeled as:

$$t_{failure} = t_{initiation[chloride]} + \frac{Thickness(mils)}{CorrosionRate(mils/year)}$$

Where: $T_0$          =      Initial Thickness (mils)
         Thickness      =      $T_0 - 0.04*t_{init[chloride]}$ [mils]
         Corrosion Rate ($R_{Cl-}$)      =      Calculated

**Case 3: IF $t_{failure}$ [Cl⁻] ≥ $t_{initiation}$ [Carbonation]**

The third case for failure of the steel liner due to corrosion is if the carbonation front reaches the steel liner prior to the failure of the steel line due to chloride. This is particularly critical, because the corrosion rates subsequent to chloride induced depassivation are equivalent to the minimum in the majority of cases, as opposed to the corrosion rate due to carbonation, i.e. 0.04 mils/year vs. 10 mils/year.

In this case, the failure time was modeled as failure due to carbonation:

$$t_{failure} = t_{initiation[carbonation]} + \frac{Thickness(mils)}{CorrosionRate(mils/year)}$$

Where the thickness of the steel liner is calculated subsequent to corrosion after the chloride induced depassivation when the carbonation front reaches:

$$T_o - \left[ \left( t_{initiation[carbonation]} - t_{initiation[Cl]} \right) \cdot R_{Cl} + \left( t_{initiation[Cl]} \cdot 0.04 \right) \right]$$

Then, the failure time can be calculated as :

$$t_{failure} = t_{initiation[carbonation]} + \frac{T_o - \left[ \left( t_{initiation[carbonation]} - t_{initiation[Cl]} \right) \cdot R_{Cl} + \left( t_{initiation[Cl]} \cdot 0.04 \right) \right](mils)}{10(mils / year)}$$

This model accounts for the corrosion prior to chloride induced depassivation, the corrosion between the initiation time to carbonation and initiation time of chloride induced corrosion, and finally the corrosion due to carbonation.

**Corrosion Rate Distribution**

It was determined that use of a corrosion rate distribution is applicable to address the variability in the corrosion rates in the passive state of steel in contact with concrete as well as other conditions that may contribute to localized general corrosion, e.g. galvanic, albeit with a lower probability. It is a practical assumption the corrosion of the carbon steel varies across the steel/concrete interface when these conditions are taken into account. Several conditions were taken into account in the development of the distribution used for the corrosion rate, shown in Fig. 5 with the corresponding passive current density.

| Quantiles of Corrosion Rates (mpy) | | | I corr ($\mu A/cm^2$) |
|---|---|---|---|
| 100.0% | maximum | 0.44978 | 0.983086 |
| 99.5% | | 0.23641 | 0.516722 |
| 97.5% | | .15527 | 0.339374 |
| 90.0% | | 0.09727 | 0.212603 |
| 75.0% | quartile | 0.06418 | 0.140278 |
| 50.0% | median | 0.04058 | 0.088696 |
| 25.0% | quartile | 0.02590 | 0.05661 |
| 10.0% | | 0.01769 | 0.038665 |
| 2.5% | | 0.01253 | 0.027387 |
| 0.5% | | 0.01059 | 0.023147 |
| 0.0% | minimum | 0.01 | 0.021857 |
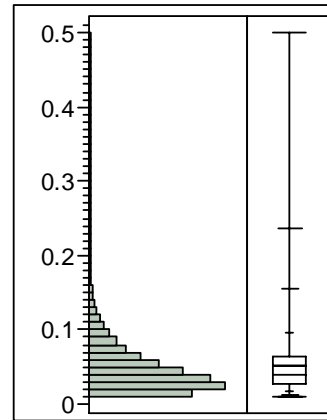


**Fig. 5:Distribution of Corrosion Rates**

Firstly, the corrosion rate of steel in contact with the concrete vault, assumed to be quality concrete, is expected to be in a "passive" state. Passivity is the state exhibited by the metal in which corrosion is limited by the diffusion of reactants through a tenacious oxide film. However, the "passive current densities" that are indicative of a steady state corrosion rate will vary depending on the specific conditions including localized conditions on the tank surface. Although the steady state corrosion rate is largely disregarded for operational conditions, it must be addressed for the geologic time-frames that are of interest for performance assessment calculations. The passive current density can be calculated utilizing Faraday's Law which relates the corrosion rate to the current density dependent upon the material:

$$CR = K_1 \frac{i_{cor}}{\rho} EW$$

Where: CR   =   corrosion rate (mpy)
       $K_1$   =   0.1288 (mpy·g/μA·cm)
       $i_{cor}$   =   current density ($\mu A/cm^2$)
       r   =   density ($g/cm^3$)
       EW   =   equivalent weight (atomic weight/valence)

The passive current densities vary from 0.02 $\mu A/cm^2$ to 1 $\mu A/cm^2$ with the broad majority in the range between 0.04 ~ 0.2 $\mu A/cm^2$. These values are consistent with literature data, of which the primary sources contends a passive current density of near 0.01 $\mu A/cm^2$ for buried steel/concrete structures.[8] However, there are various passive current densities reported depending upon the specific concentration of the pore water tested from 0.01 – 10 $\mu A/cm^2$.[2,17] The relevant passive current density used for input into the PA are those for buried steel/concrete structures. In addition, these passive current densities and the electrochemical potential regimes in which corrosion can occur is reported to be exacerbated by the presence of the chloride ion, but the SRS chloride concentrations are significantly lower than those in the literature, thereby indicating a consistent passive current density.[8] The minimum passive current density used for the calculation is twice the reported values for buried structures.

The distribution of the corrosion rates is assumed to account for some of the localized areas within the tank surface that may be subject to greater than the median corrosion rate of 0.04 mpy. For example, there are locations within the tank where pumps anchored to the carbon steel bottom with stainless steel anchors will be grouted in place which may lead to galvanic corrosion currents in the slight areas of contact. The galvanic corrosion currents between stainless steel and carbon steel are known to be negligible in experimental time-frames, but were considered for this analysis due to the time-frames involved. The current density contributions from the galvanic currents particularly for a passive carbon steel are reported to stabilize near 0.2 $\mu A/cm^2$.[18] The area which the stainless steel contacts the carbon steel is a minute fraction of the entire surface of the tank bottom. Another potential area of higher than nominal passive current densities is the welded regions of the bottom plate. Once again, the welded areas and the subsequent heat-affected zones of those welds where microstructural features may lead to greater than nominal corrosion is small in comparison to the total surface area of the nominal base metal exposed. As such, the distribution of corrosion rates is expected to encompass these regions appropriately.

The implication of the potential for a high corrosion rate to be chosen during the simulation is the occurrence of premature corrosion prior to the initiation of carbonation or chloride induced depassivation. As such, a "Case 0" was calculated as:

$$t_f = T_0 / Rnd(0.04)$$
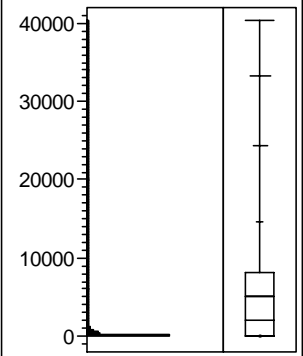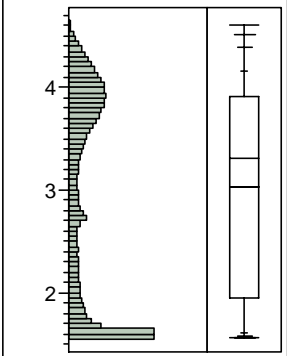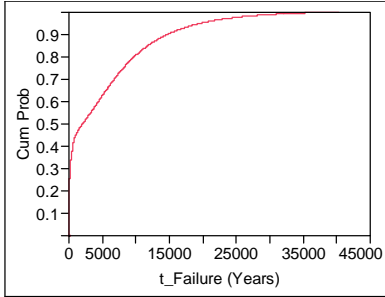
where: $t_f$          =   time to failure (years)
       $T_0$          =   Initial thickness (mils)
       Rnd (0.04)    =   Corrosion rate chosen from distribution

when the tank fails due to general corrosion before the initiation of either corrosion mechanism. The time to failure is then used as input to determine the interaction with Cases 1-3 as presented before. It is expected that the thicker sections of concrete may fail via this mode since the time required for carbonation/chloride to reach the steel/concrete interface will be longer than the initial corrosion rate. When this is not the case, one of the initial cases will apply.

**RESULTS**

The results of the life estimation are presented in Table 2 as quantiles, log-time to failure, and the cumulative distribution plots.  The results can be interpreted in several ways.  The quantiles may be used as input for modeling the outflow of contaminants from the tanks by (1) using the median value as a best estimate for failure times under the assumption of complete consumption, (2) using a figure of merit for percentage breached for a "patch" type models which will progressively fail the tank and assume that past a critical percentage breached, the tank no longer acts as a barrier to contaminant escape, or (3) using the entire distribution in any stochastic modeling.  The progressive breaching of the tank steel is likely the most representative of the natural phenomena of corrosion of the steel.  However, choosing a figure of merit as input for complete permeation is a challenge due to the spatial resolution necessary for consequence modeling.

**Table 2: Time to Failure for Tank Steel**

| Time to Failure | Log Time to Failure: | CDF Plot |
|---|---|---|



**Quantiles** (Time to Failure)

| 100.0% | maximum | 40391 |
|---|---|---|
| 99.5% | | 33244 |
| 97.5% | | 24287 |
| 90.0% | | 14610 |
| 75.0% | quartile | 8104 |
| 50.0% | median | 2010 |
| 25.0% | quartile | 90 |
| 10.0% | | 41 |
| 2.5% | | 38 |
| 0.5% | | 37 |
| 0.0% | minimum | 37 |

**Quantiles** (Log Time to Failure)

| 100.0% | maximum | 4.6063 |
|---|---|---|
| 99.5% | | 4.5217 |
| 97.5% | | 4.3854 |
| 90.0% | | 4.1647 |
| 75.0% | quartile | 3.9087 |
| 50.0% | median | 3.3031 |
| 25.0% | quartile | 1.9521 |
| 10.0% | | 1.6091 |
| 2.5% | | 1.5801 |
| 0.5% | | 1.5684 |
| 0.0% | minimum | 1.5624 |

**Moments** (Time to Failure)

| Mean | 5161.4916 |
|---|---|
| Std Dev | 6847.8707 |
| Std Err Mean | 6.1669434 |
| upper 95% Mean | 5173.5786 |
| lower 95% Mean | 5149.4046 |
| N | 1233023 |

**Moments** (Log Time to Failure)

| Mean | 3.0267292 |
|---|---|
| Std Dev | 0.9836818 |
| Std Err Mean | 0.0008859 |
| upper 95% Mean | 3.0284655 |
| lower 95% Mean | 3.0249929 |
| N | 1233023 |

**Failure Mode Frequency**

| Level | Count | Prob |
|---|---|---|
| 0 | 709530 | 0.57544 |
| 1 | 523493 | 0.42456 |
| Total | 1233023 | 1.00000 |

The stochastic analysis elucidated insights into the controlling mechanisms of failure  The failure times, as presented in previous sections, are a function of the diffusion coefficients of oxygen and/or $CO_2$, thereby controlling the failure times.  The analyses were based upon the assumption that carbonation was the most aggressive mechanism of corrosion of the tank liner due to the loss of the high pH environment,

and that chloride may induce depassivation on the steel surface, but is still dependent upon the oxygen diffusion to drive the corrosion reaction.  The relative effects of carbonation and chloride induced corrosion as a function of diffusion coefficient can be seen by comparing the median values of failures for each of the conditions.  The results suggest that the carbonation rates are the critical factor in controlling the life estimation.  Once the carbonation front has reached the steel liner, the liner is essentially consumed within a time frame of 50 years nominally.  As such, the recommendations for failure time use in stochastic modeling for contaminant escape are critically linked to the diffusion coefficients.  The diffusion coefficient for oxygen through the concrete is not as critical until very high diffusion rates with minimal amounts of concrete cover.

It is important to recognize that the diffusion coefficients may change over the course of time.  One driver for change in the diffusion rates may be due to crack development in the concrete structures, for example, due to rebar corrosion. The concrete vaults of the high level waste have an extensive network of rebar to enhance the structural integrity of the concrete.  The corrosion of the rebar may impact the life estimates of the tank steel for their closure performance assessment.  The rebar is generally protected by a passive layer when in contact with the alkaline environment of the concrete.  However, passivity can be lost through carbonation or through chloride induced film breakdown.  The expansion of the corrosion products on the surface of the rebar can cause substantial stress on the concrete leading to cracking and potentially spalling of the concrete structure.  This cracking potentially then minimizes the concrete cover thickness, as well as potentially increases the diffusion coefficients of ions through the structures.  However, a comprehensive review of the rebar in the waste tanks and a visual assessment of the concrete vaults surrounding the waste tanks concluded that degradation of the concrete due to rebar corrosion was improbable.[19]  The visual inspection of the concrete condition focused on a matrix of eight attributes: (1) general condition, (2) cracks, (3) scaling, (4) spalling, (5) corrosion/chemical attack, (6) stains, (7) exposed steel, and (8) repair.

## ACKNOWLEDGEMENTS

**REFERENCES**

[1] ASTM Standard A285, "Standard Specification for Pressure Vessel Plates, Carbon Steel, Low- and Intermediate-Tensile Strength," American Society for Testing of Materials, (2006).

[2] B. HUET, V.L. HOSTIS, F. MISERQUE, H. IDRISSI, "Electrochemical Behavior of Mild Steel in Concrete: Influence of pH and Carbonate Content of Concrete Pore Solution," *Electrochimica Acta*, **51** (2005), pp. 172-180.

[3] C.L. PAGE and K.W.J. TREADWAY, "Aspects of the Electrochemistry of Steel in Concrete," *Nature*, **297** (1982), pp. 109-115.

[4] "Concrete Standard Engineering Specification," SB 6U, E.I. Dupont de Nemours, (1966).

[5] B.J. WIERSMA, "An Investigation of the Potential for Corrosion of the Concrete Rebar in the SRS Waste Tanks," WSRC-TR-93-185, Westinghouse Savannah River Company, July 1993.

[6] Corrosion of Metals in Concrete, ACI Journal, January-February 1985, p. 3-32.

[7] P. NOVAK, R. MALA, L. JOSKA, "Influence of Pre-Rusting on Steel Corrosion in Concrete," *Cement and Concrete Research*, **31**, 589 (2001).

[8] C. ANDRADE, I. MARTINEZ, M. CASTELLOTE, P. ZULOAGA, "Some Principles of Service Life Calculations of Reinforcements and In-Situ Corrosion Monitoring by Sensors in the Radioactive Waste Containers of El Cabril Disposal (Spain), Journal of Nuclear Materials, **358** (2006) 82-95.

[9] K.C. CLARK, "Time to Corrosion of Reinforcing Steel in Concrete Slabs," Vol. 3. Performance AGTER 830 Daily Salt Applications, Federal Highway Administration Report No. FHWA-RD-76-70, NIST PB-258 446.

[10] R.N. STROM, D.S. KABACK, "Groundwater Geochemistry of the Savannah River Site and Vicinity," WSRC-RP-92-450, Westinghouse Savannah River Company (1992).

[11] V.G. PAPADAKIS, M.N. FARDIS, "A Reaction Engineering Approach to the Problem of Concrete Carbonation," AICHE Journal, **35** (10) (1989).

[12] J.C. WALTON, L.E. PLANSKY, R.W. SMITH, "Models for Estimation of Service Life of Concrete Barriers in Low-Level Radioactive Waste Disposal," NUREG-CR-4552, (1990).

[13] H.H. UHLIG, Corrosion and Corrosion Control, John Wiley & Sons, (1971), p. 99.

[14] "Concrete Standard Engineering Specification," Specification 3552, E.I. Dupont de Nemours, (1966).

[15] R.S. WALTZ, W.R. WEST, "Annual Radioactive Waste Tank Inspection Program (U)," WSRC-TR-2005-00276, Washington Savannah River Company, (2005).

[16] J.C. WALTON, "Performance of Intact and Partially Degraded Concrete Barriers in Limiting Mass Transport," NUREG-CR5445, (1992).

[17] C. ANDRADE, et. al. "Electrochemical Behaviour of Steel Rebars in Concrete: Influence of

Environmental Factors and Cement Chemistry," Electrochimica ACTA **46** (2001) 3905.

[18] S. QIAN, D. QU, and G. COATES, "Galvanic Coupling between Carbon Steel and Stainless Steel Reinforcements," NRCC-48162, National Research of Canada, (2005).

[19] B.J. WIERSMA and M.S. SHURRAB, "A Visual Assessment of the Concrete Vaults which Surround Underground Waste Storage Tanks," WSRC-TR-93-761, Westinghouse Savannah River Company, (1993).